CMT Ceramics in Modern Technologies
Techna Group srl

Search for Novel Use of Waste Gypsum: Part 1. Detailed Investigation on Waste Gypsum Phosphatization

Akari Takeuchi[a]*, Takuma Hikida[a], Hiroko Hamano[a], Masamoto Tafu[b], Masanori Kikuchi[c]
[a]Department of Chemistry, Faculty of Science, Shinshu University, Matsumoto, Nagano, Japan; [b]National Institute of Technology, Toyama College, Toyoma, Toyama, Japan; [c]Bioceramics Group, Research Center for Functional Materials, National Institute for Materials Science, Tsukuba, Ibaraki, Japan

Phosphatization of waste gypsum (w-Gyp) was investigated in detail to search novel use for a recycling of waste gypsum boards as spherical beads composed of various calcium phosphates. The component of the w-Gyp powder was gypsum ($CaSO_4 \cdot 2H_2O$) with some inorganic and organic impurities. The w-Gyp heated at 120 °C for 24 h was bassanite ($CaSO_4 \cdot 0.5H_2O$) single phase as the same as the reagent gypsum. Mixture of heated w-Gyp and ion-exchanged water was successfully hardened as spherical gypsum beads in vegetable oil. The degree of phosphatization of w-Gyp and crystal phases of calcium phosphates formed were affected by treatment conditions, pH, temperature and reaction period. The w-Gyp was barely phosphatized in acidic pH with positively temperature depended increasing in reacted amounts. The phosphatization was completed in 6 to 24 h under neutral conditions and in 1 to 6 h under basic conditions. Dicalcium phosphate dihydrate (DCPD) could firstly be formed in all conditions and it changed into dicalcium phosphate anhydrous (DCPA) by dehydration of DCPD at over 60 °C. Under higher pH conditions, DCPA or DCPD was subsequently converted into hydroxyapatite, the most stable calcium phosphate in water. During the conversion, β-tricalcium phosphate (β-TCP) was also formed by the presence of Mg^{2+}, a stabilizer of β-TCP. Spherical beads consisting of these calcium phosphates were prepared from spherical beads of the w-Gyp.

Keywords: Waste gypsum; Calcium sulfate; Calcium phosphate; Bead; Hydrothermal treatment.

1. Introduction

A gypsum board is one of the most common building materials and has been used all over the world because of its ease of fabrication and workmanship as well as several useful properties such as fire-resistance and sound insulation. However, massive use of gypsum boards leads a serious problem in disposal of waste gypsum boards, more than 1,000,000 tons a year in Japan at present. Further, the Gypsum Board Association Japan estimates that it will increase more than 3,000,000 tons in 2047 and continue to increase gradually by 2068 [1]. Therefore, a recycling of waste gypsum boards must be promoted immediately. One of the simplest ways for the recycling is the reproducing of gypsum boards using calcium sulfate hemihydrate derived from heated waste gypsum, calcium sulfate dihydrate; however, waste gypsum boards have been only partially utilized because of inferior qualities of the refurbished products [2, 3]. Up to now, no effective recycling ways for the waste gypsum disposal have been found, even many methods have been studied on that in several decades [2-6].

Hydroxyapatite (HAp) and related calcium phosphates are well known as materials for environmental purification. Hydroxyapatite has an ion-exchange ability, thus it has been investigated as materials for removal of heavy metal ions and radioactive strontium ions from water [7-13]. Dicalcium phosphate dihydrate (DCPD) and other calcium phosphates have also been investigated for removal of fluoride ion [14-17]. These calcium phosphates can be easily prepared through a precipitation reaction from aqueous solution, and preparation methods of HAp using gypsum as a starting material have also been documented [18-22]. Furuta *et al*. reported that a waste gypsum, used as molds for slip or pressure casting in the ceramic industry, would be used as a starting material for HAp preparation [18]. They phosphatized the waste gypsum by a hydrothermal treatment in $(NH_4)_2HPO_4$ aqueous solution at various temperatures from 50 to 190 °C. They also reported the feasibility of the prepared HAp for lead ion removal [7]. Yasuike *et al*. [21] reported a HAp preparation using the gypsum collected from waste gypsum boards, the waste gypsum, by a phosphatization in the phosphate-bearing solution, harvested from a sewage sludge ash under a basic condition. They also examined its removal ability of lead, cadmium and fluoride ions. Both researches focused on HAp preparation and its application for harmful ion removal, and successfully proposed the recycling method of the waste gypsum. However, the waste gypsum theoretically is phosphatized not only to HAp but also to various calcium phosphates, having a variety of chemical properties under various levels of pH, and control of calcium phosphate phases from the waste gypsum will be applied to environmental purification materials in broader situations. In addition to that, spherical beads would improve handling and filtration properties than powder, even though powder generally has higher specific surface area that is a great advantage for ion removing reactions.

The aim of the present study is to establish a fabrication method

* *Corresponding author*
E-mail address: taakari@shinshu-u.ac.jp

https://doi.org/10.29272/cmt.2019.0013
Received August 9, 2019; Received in revised form September 4, 2019; Accepted September 5, 2019

of spherical beads composed of various calcium phosphates from spherical beads of the waste gypsum by elucidating phosphatization conditions of the waste gypsum in detail.

2. Materials and Methods

2.1. Pre-treatment of waste gypsum powder

A waste gypsum powder, w-Gyp, was collected from powdered waste gypsum boards by removing fine fibers of lining paper with a stainless steel sieve of 475 μm in mesh size. The w-Gyp was then heat-treated at 120 °C in a drying oven (OF-300B, AS ONE Corp., Osaka, Japan) for 24 h, generally believed dehydration conditions of gypsum, $CaSO_4 \cdot 2H_2O$, to be bassanite, $CaSO_4 \cdot 0.5H_2O$, and the heated w-Gyp is denoted as hw-Gyp. Reagent grade bassanite powder (c-Bas, calcium sulfate, calcined, CP grade, Nacalai Tesque, Inc., Kyoto, Japan) was mixed with ion exchanged water and dried to be hydrated c-Bas powder, c-Gyp. The w-Gyp, hw-Gyp and c-Bas powders were characterized by an ion chromatography (IC), a scanning electron microscopy (SEM) and an X-ray diffraction (XRD) analyses as described in section 2.4.

2.2. Preparation of gypsum pastes and beads

A hw-Gyp paste was prepared by mixing the hw-Gyp and ion exchanged water at a water-to-powder ratio of 1.26. The hw-Gyp paste was then added into 200 mL of vegetable oil (grape-seed oil, J-OIL MILLS Inc., Tokyo, Japan) in 300 mL-glass-beaker stirred with a three-bladed stainless steel propeller at a rotation of 500 per minute at room temperature for 1 h to be hardened as spherical beads, w-Beads. The gypsum beads obtained were then harvested from the oil by filtration through the stainless steel sieve. The beads were washed in acetone (GR grade, Nacalai Tesque, Inc., Kyoto, Japan) with an ultrasonication for 10 minutes twice followed by an ultrasonic washing in ion-exchanged water for 10 minutes twice to remove the vegetable oil, and dried at 60 °C for 24 h. A control paste, c-Bas paste, and beads, c-Beads, were prepared using the c-Bas by the same method except for the water-to-powder ratio of 1.00. The powder to water ratios and hardening time were determined from preliminary tests for mixing and hardening. The dried beads were analyzed by the XRD, SEM and thermogravimetry-differential thermal analysis (TG-DTA) as described in section 2.4.

2.3. Phosphatization of waste gypsum powder and beads

Acidic, 4 in initial pH, and basic, 8 in initial pH, phosphate bearing solutions were prepared by dissolving respective guaranteed reagents of $NH_4H_2PO_4$ (Guaranteed Reagent FUJIFILM Wako Pure Chemical Corp, Osaka, Japan) and $(NH_4)_2HPO_4$ (Guaranteed Reagent FUJIFILM Wako Pure Chemical Corp, Osaka, Japan) into ion-exchanged water at a concentration of 1 mol/L. These solutions were mixed to prepare neutral, 7 in initial pH, solution. One gram of the powder was added to a stainless steel autoclave with a Teflon® liner (internal volume: 25 mL, Shikokurika Co., Ltd., Kochi, Japan) with 20 mL of one of the solutions and hydrothermally treated in a drying oven at 100 or 200 °C. The same amounts of the powder and phosphate bearing solution were heat-treated in screw-top glass bottle (internal volume 50 mL, AS ONE Corp., Osaka, Japan) at 50 °C. The c-Gyp powder was also phosphatized as a control.
After the treatment for up to 72 h, powder and liquid were separated with a centrifuge at 500 g for 5 min (himac CT4D, Hitachi Koki Co., Ltd., Tokyo, Japan). The powder was washed trice with ion-exchanged water, dried at 60 °C for 24 h, and analyzed by the XRD and IC. Values of the solution pH before and after phosphatization were measured at room temperature with a handheld pH meter (D-52, equipped with a combination pH electrode, 9625-10D, Horiba Ltd., Kyoto, Japan).
The gypsum beads were also phosphatized for 72 h in the same way as that for powder and analyzed by the XRD.

2.4. Characterizations

2.4.1. Quantitative chemical analyses

Cationic and anionic compositions of samples were determined by the IC. Each sample was dissolved in 0.1 mol/L-HNO_3 (Guaranteed Reagent, FUJIFILM Wako Pure Chemical Corp., Osaka, Japan) and analyzed using a high-performance liquid chromatograph system (LC-10A series, Shimadzu Corp., Kyoto, Japan) consisted of a SCL-10A system controller, LC-10 CE pump, SIL-10A auto-injector, CTO-10A column oven, and CDD 6A conductivity detector linked to a Chromato-PRO data integrator (Run Time Corp., Kanagawa, Japan). Concentrations of cations in the solutions were determined using a cationic column, Shodex® IC YS-50 (Showa Denko K.K., Tokyo, Japan) with eluting solution of 4.0 mmol/L-methanesulfonic acid (2.0 mol/L-methanesulfonic acid solution for ion chromatography, FUJIFILM Wako Pure Chemical Corp., Osaka, Japan) at a flow rate of 0.65 mL/min, and those of anions were determined using an anionic column, Shim-Pack IC-A1 (Shimadzu Co., Kyoto, Japan) with a mixed aqueous solution of 6.0 mmol/L-boric acid, 18.0 mmol/L-D(-)-mannitol and 7.5 mmol/L tris-(hydroxymethyl)-aminomethane (Guaranteed Reagent, FUJIFILM Wako Pure Chemical Corp., Osaka, Japan) at a flow rate of 0.5 mL/min.

2.4.2. Crystal phase identification

Inorganic crystal phases of the samples were identified with powder X-ray diffractometer (Ultima IV, Rigaku Corp., Tokyo, Japan) using graphite-monochromatized CuKα radiation generated at 40 kV and 40 mA by a continuous scanning mode at a step size of 0.02 ° and a scanning rate of 2.00 °/min.

2.4.3. Morphologies

The samples were fixed on brass sample holders with an electroconductive carbon tape (Nisshin EM Co., Ltd., Tokyo, Japan) and/or an electroconductive carbon paste (DOTITE XC-12, JEOL Ltd., Tokyo, Japan), and were coated with osmium at 10 mA for 20 s (osmium coater, Neoc-AN, Meiwafosis Co., Ltd., Tokyo, Japan). Whole and surface morphologies of the samples were observed with a field emission-scanning electron microscope (FE-SEM, JSM-7600F, JEOL Ltd., Tokyo, Japan) at an accelerating voltage of 15 kV.

2.4.4. Thermal property analyses

Thermal properties of the w-Beads were analyzed by a thermogravimetric-differential thermal analysis system (SII6300, Seiko Instruments, Inc., Chiba, Japan). The w-Beads were placed in a platinum pan, and TG-DTA data were collected from 25 to 1000 °C at a heating rate of 10 °C·min^{-1} under an air atmosphere. Alpha-alumina powder was used as a reference material for DTA.

3. Results and Discussion

Figure 1 shows images given by a common digital camera (i) and FE-SEM (ii) of the hw-Gyp and c-Bas. The hw-Gyp demonstrated dusty color in comparison to the c-Bas (Fig. 2(i)) and contained some fine paper fibers even after sieving. The hw-Gyp consisted of plate-like particles of 0.1-5 μm in size as shown in Fig. 1(ii)(a) and was similar to that of the waste gypsum reported by Kojima *et al.* [3]. The c-Bas was also composed of plate-like particles of 5-10 μm in size, on which finer particles aggregated, as illustrated in Fig. 1(ii)(b).

(i) Macroscopic images

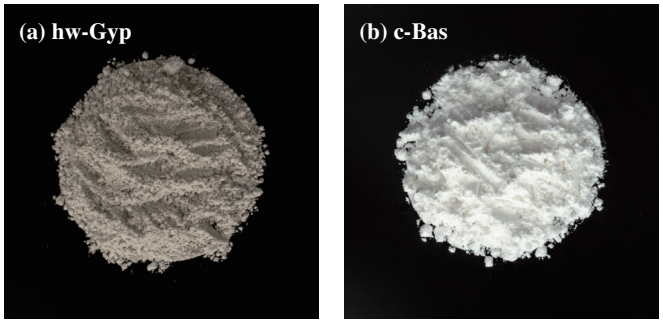

(ii) SEM images

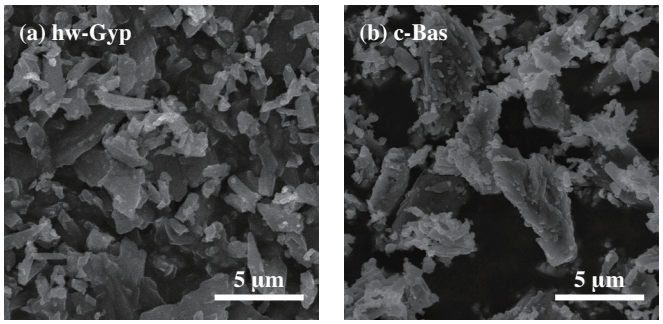

Figure 1. Macroscopic (i) and SEM (ii) images of hw-Gyp and c-Bas powders.

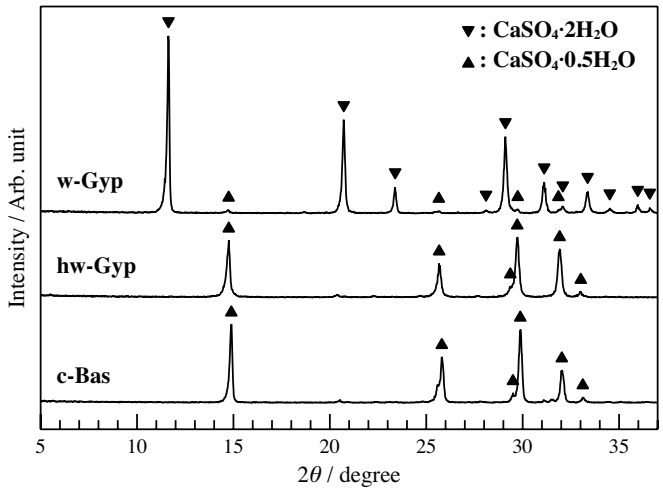

Figure 2. Powder X-ray diffraction patterns of w-Gyp, hw-Gyp and c-Bas.

Figure 2 shows XRD patterns of the w-Gyp and hw-Gyp with the c-Bas as a reference. Peaks for the w-Gyp were assigned to gypsum ($CaSO_4 \cdot 2H_2O$, ICDD-33-311) containing a small amount of bassanite ($CaSO_4 \cdot 0.5H_2O$, ICDD-41-224). The hw-Gyp was a single phase of bassanite and was the same crystal phase as the c-Bas.

Chemical compositions of the w-Gyp and c-Bas, determined by the IC, were listed in Table 1. Main components of the w-Gyp and c-Bas were, of course, calcium and sulfate ions. Sodium, ammonium, potassium, magnesium, fluoride and phosphate ions were only detected in the w-Gyp. Though origins of these impurities were not specified from the results, they ought to derive from raw materials of gypsum boards, i.e., gypsum minerals, recycled gypsum boards, some additives during fabrication process and/or other architectural materials mixed during demolition of buildings.

Generally, flowability of powder is decreased with decreasing in particle size in the range of 2-30 μm in diameter [23]. The particle sizes of the presently used powders would be within the range. Further, flowability would also be decreased by the formation of column-like gypsum crystals as well as sulfate ion dissolution in the water phase due to reaction between powder and water. This phenomenon occurred in both powders, but of course, powder with smaller particle size has larger specific surface area, i.e., reaction sites, than that with larger particle size. According to the present results, the larger water-to-powder ratio for the hw-

Table 1. Chemical compositions of w-Gyp and c-Bas. ND: Not detected.

	w-Gyp (mol%)	c-Bas (mol%)
Na^+	4.68 ± 0.42	ND
NH_4^+	0.107 ± 0.226	ND
K^+	0.188 ± 0.067	ND
Mg^{2+}	0.363 ±0.070	ND
Ca^{2+}	94.6 ± 0.3	100
F^-	0.766 ± 0.044	ND
SO_4^{2-}	97.0 ± 0.1	100
PO_4^{3-}	2.18 ± 0.08	ND

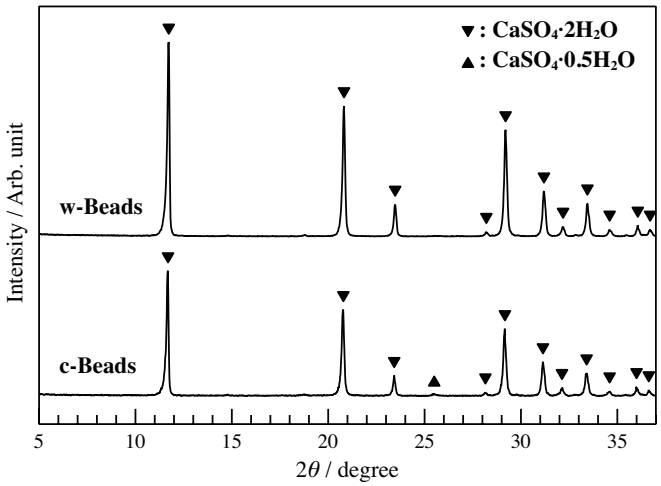

Figure 3. Powder X-ray diffraction patterns of w-Beads and c-Beads.

(i) Macroscopic images

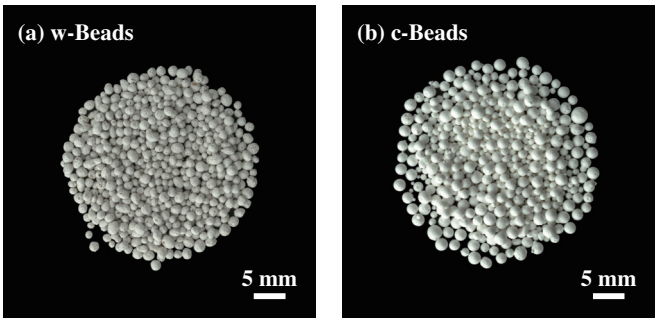

(ii) SEM images

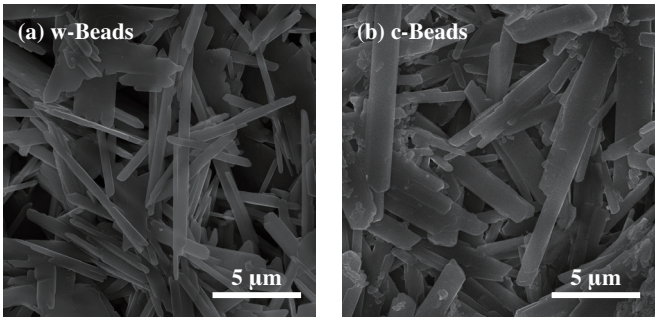

Figure 4. Macroscopic (i) and SEM (ii) images of w-Beads and c-Beads.

Gyp determined by a preliminary handling tests than that for the c-Bas can be ascribed to the particle size and remained fine paper fibers.

Figure 3 illustrates the XRD patterns of the w-Beads and c-Beads. The w-Beads was identified as a gypsum single phase, but the c-Beads contained small amounts of bassanite other than gypsum. This means that smaller particle size reacted better than larger one as described above. Naked-eye observations of the w-Beads and c-Beads shown in Fig. 4(i) presented that the size of both beads was approximately 1 mm in diameter. Note that the hw-Gyp paste at a water-to-powder ratio of 1.00 in the preliminary run did not form spherical beads by the present method because of low flowability. The entanglements of needle-like crystals, that is typical for hardened gypsum [24], were observed in both beads by the SEM (Fig. 4(ii)), whereas the features of them were slightly different. Crystals in the w-Beads were thinner than those in the

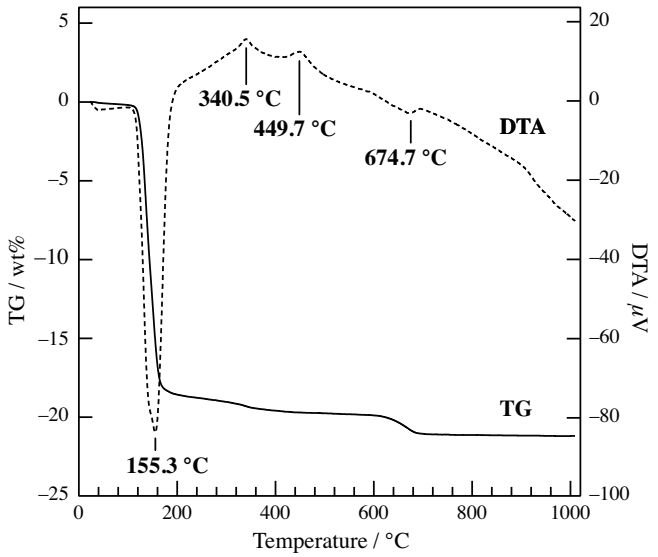

Figure 5. Thermogravimetry and differential thermal analyses curves for w-Beads. (Solid line: TG, Dotted line: DTA)

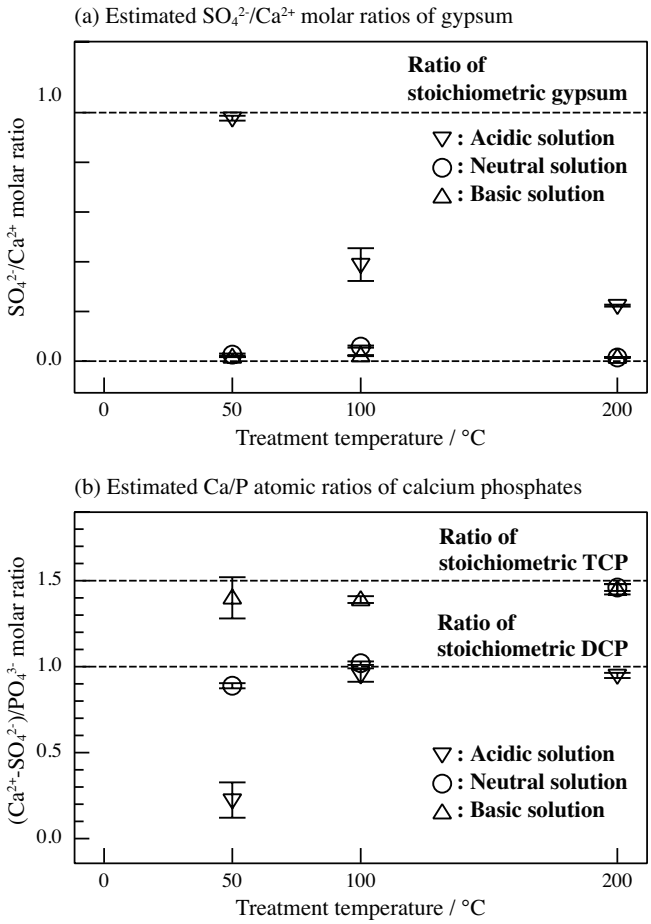

Figure 6. Estimated SO_4^{2-}/Ca^{2+} molar ratios of gypsum and Ca/P atomic ratios of calcium phosphates in w-Gyp phosphatized for 72 h.

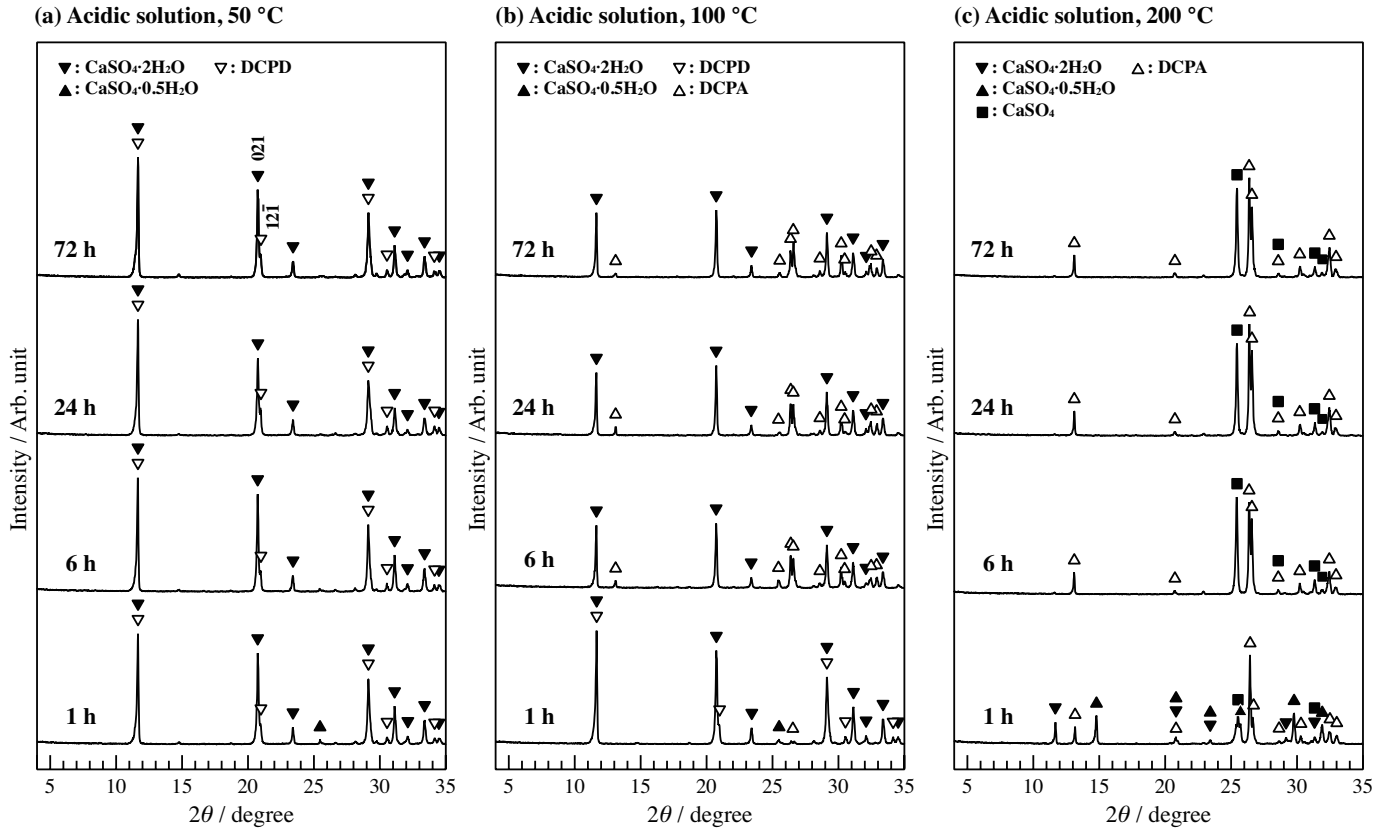

Figure 7. Powder X-ray diffraction patterns of w-Gyp after phosphatization in acidic ammonium phosphate salt solution at 50, 100 or 200 °C for up to 72 h.

c-Beads, because the smaller-particles of the hw-Gyp allowed much faster hydration reaction than the larger-particle of c-Bas [3]. Furthermore, crystals in the w-Beads entangled somewhat more sparsely than those in the c-Beads due to greater water amounts in the hw-Gyp paste. These differences resulted in the weakness of the w-Beads as compared with the c-Beads in the preliminary diametral tensile strength test for the w-Gyp disk fabricated by filling the pastes in a stainless steel mold via the same conditions demonstrated 0.6 times higher than disks composed of the c-Gyp (data was not shown).

Figure 5 shows the TG and DTA curves of the w-Beads. The first endothermic peak and significant weight loss, from 100 to 200 °C, were attributed to a dehydration of gypsum to anhydrite III [25-28] through bassanite confirmed as a small shoulder. The following exothermic peak at 340.5 °C was assigned to a transformation of anhydrite III to anhydrite II [29, 30]. The exothermic peak at 449.7 °C could be a decomposition of organic substances in waste gypsum boards, e.g. paper fiber, adhesive agent and/or other organic additives [31]. The endothermic peak with obvious weight loss at 674.7 °C was attributed to a decomposition of calcium carbonate, that is known as one of additives in waste gypsum boards [27, 28]. From this result, the w-Beads contained some organic impurities and calcium carbonate other than gypsum, even though these were not detected in the XRD and IC analyses.

Insoluble substances in the w-Beads after the phosphatization were calcium sulfates and calcium phosphates except for monocalcium phosphates; therefore, molar ratios of calcium sulfates in the precipitate after the phosphatization were estimated by molar ratios of SO_4^{2-}/Ca^{2+}, and Ca/P atomic ratios of calcium phosphates in the precipitates were approximated by molar ratios of $(Ca^{2+}–SO_4^{2-})/PO_4^{3-}$ because the same molar SO_4^{2-} and Ca^{2+} were theoretically dissolved in the liquid phase by the phosphatization and those Ca^{2+} were precipitated as calcium phosphates as well as calcium sulfates. Those in the w-Gyp phosphatized for 72 h, determined from the results of the IC, were summarized in Fig. 6. Slight phosphatization of the w-Gyp at 50 °C in the acidic solution and temperature dependent progress of the phosphatization was suggested from the estimated calcium sulfate amounts, nearly 1. Almost complete phosphatizations of the w-Gyp in the neutral and basic conditions were also suggested from the Fig. 6(a). Figure 6(b) demonstrated that Ca/P atomic ratios in the precipitates increased with increasing in initial pH.

Values of pH for each condition after the phosphatization were summarized in Table 2. The phosphatization generally decreased pH values of the reaction solutions with time due to dissolution of sulfate, a stronger acid than phosphates.

Figure 7 summarizes XRD patterns of the w-Gyp after phosphatization in the acidic solution at 50, 100 and 200 °C for 1, 6, 24 and 72 h. Powder X-ray diffraction patterns of the w-Gyp in the acidic solution at 50 °C shown in Fig. 7(a) demonstrates detection of peaks besides gypsum, assigned to dicalcium phosphate dihydrate (DCPD, brushite, ICDD-1-72-713), from the initial stage of phosphatization, at 1 h after the treatment. Peak intensity ratio of $12\bar{1}$ diffraction of DCPD to 021 diffraction of gypsum was maintained virtually constant up to 72 h, and it meant that the phosphatization reaction barely proceeded in the acidic pH at 50 °C. Estimated amount of calcium phosphates at 72 h after the phosphatization, 2.3% in mol, was agreed with the XRD results; however, the estimated Ca/P ratio, 0.2 ± 0.1, was smaller than stoichiometric value of DCPD, 1.0, that was to say, phosphate ions were excess in the precipitate. These results suggested that a formation of ardealite (Ard, $Ca(SO_4)_{1-x}\cdot(HPO_4)_x\cdot 2H_2O$ with $x \approx 0.5$) [32]. Relative amount of ardealite to DCPD can be approximated as following equation;

$$\mathrm{Ard} = \frac{2\cdot\mathrm{DCPD}\cdot(1-\mathrm{A})}{\mathrm{A}} \quad (1)$$

where $A = (Ca^{2+}–SO_4^{2-})/PO_4^{3-}$ molar ratio.

From the equation, DCPD to ardealite molar ratio was approximated to 1:7, and ardealite of approximately 3-4% in mol to gypsum could form during the reaction.

Figure 7(b), summary of 100 °C treatments, illustrates detection of dicalcium phosphate anhydrous (DCPA, monetite, ICDD-1-70-360) as well as DCPD after 1-h treatment, and subsequent increasing of DCPA with disappearance of DCPD peaks at 6 h after treatment. The gypsum remained even after 72-h treatment although the smaller estimated gypsum ratio at 100 °C indicated the more proceeded phosphatization than at 50 °C. From the equation 1, estimated DCPD to ardealite molar ratio was 10:1, and ardealite of less than 2% in mol to gypsum could form during the reaction.

Treatment at 200 °C induced dehydration of gypsum to anhydrite (gypsum anhydrous, ICDD-1-80-6362) as detected in Fig. 7(c). All detected calcium phosphates in this condition was DCPA. Although the smaller SO_4^{2-}/Ca^{2+} molar ratios in Fig. 6 indicated the more proceeded phosphatization reaction, the reaction of calcium phosphate formation seemed to achieve equilibrium after 24 h on the basis of the XRD result in Fig. 7(c). From the equation 1, estimated DCPD to ardealite molar ratio was 9:1, and ardealite of approximately 3% in mol to gypsum could form during the reaction.

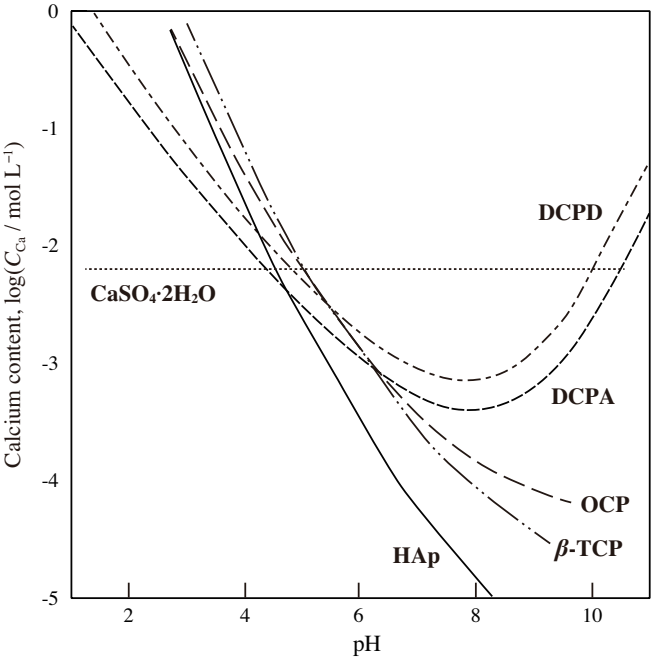

Figure 8. Solubility isotherms of gypsum, HAp and related calcium phosphates at 25 °C [20, 33-35].

Figure 8 shows the solubility isotherms vs. pH of gypsum, HAp and related calcium phosphates at 25 °C [20, 33-35] where the solubility of each compound was expressed as the molarity of Ca^{2+} in aqueous solution saturated with respect to it. Reaction of calcium phosphate formation from more soluble calcium salt, such as gypsum dihydrate, in a phosphate salt aqueous solution was known to proceed through a dissolution-reprecipitation process in which Ca^{2+} released from calcium salt and PO_4^{3-} in the aqueous solution precipitate as a calcium phosphate compound [20]. Solubility isotherms at 25 °C shows that gypsum is more insoluble than calcium phosphates under an acidic condition. Although solubilities of gypsum has a temperature gradient maximum at around 40 °C [24, 35, 36] and calcium phosphates have a negative temperature gradient [34], gypsum should be more insoluble than calcium phosphates even at 50 °C under the sulfate-phosphate acidic conditions because this temperature and the similar acidic conditions are generally used to fabricate gypsum or bassanite from apatite [23, 37]. The results of the

present study, poor proceeding of the phosphatization reaction at 50 °C in the acidic aqueous solution, were agreed with these literatures.

A small amount of DCPD formation after 50 °C treatment was in accordance with the reports that the faster crystal growth of DCPD than DCPA at normal temperature and pressure in $Ca(OH)_2$-H_3PO_4-H_2O system [33, 38], despite the most insoluble calcium phosphate under an acidic condition is DCPA as shown in Fig. 8. Under the acidic conditions, DCPD was formed during temperature elevation to the "reaction" temperatures followed by dehydration to DCPA over 60 °C [33, 39]. The lower "reaction" temperature and shorter reaction time should not sufficient to dehydrate all the DCPD formed during the temperature elevation; therefore, DCPD was detected after 1-h treatment at 100 °C. The other reaction times for 100 °C treatments as well as 200 °C treatments allowed complete dehydration of DCPD to DCPA as well as direct formation of DCPA above 60 °C.

The more proceeded phosphatization reaction at 100 °C than 50 °C was explained from an accelerated crystal growth of DCPA at higher temperature, that was to say, the acceleration of the DCPA crystal growth shifted the equilibriums of following equations to the right.

$$(\text{dissolution of } CaSO_4{\cdot}2H_2O)\ CaSO_4{\cdot}2H_2O \rightleftarrows Ca^{2+} + SO_4^{2-} + 2H_2O$$

$$(\text{precipitation of DCPA})\ Ca^{2+} + HPO_4^{2-} \rightleftarrows CaHPO_4$$

The more proceeded phosphatization reaction of gypsum decreases pH by release of sulfuric acid, and it corresponded to the lower pH after 72-h treatment at higher temperature as shown in Table 2. The most proceeded phosphatization reaction at 200 °C under the acidic condition would be explained in the same way. A dehydration of gypsum to anhydrite II [40] was also proceeded by the treatment at 200 °C.

Table 2. Values of pH for each condition after phosphatization.

	Temperature / °C		
Initial pH	50	100	200
4	3.39	2.86	2.64
7	6.54	5.75	5.31
8	6.90	5.88	6.79

Figure 9 shows XRD patterns of the w-Gyp after phosphatization in the neutral solution at 50, 100 or 200 °C for up to 72 h. Diffraction peaks of DCPD were detected as well as gypsum after 1-h treatment at 50 °C. The single phase of DCPD was obtained after 6 h (Fig. 9(a)) despite the most insoluble calcium phosphate under a neutral condition is HAp (Fig. 8). The molar ratios in Fig. 6, SO_4^{2-}/Ca^{2+}, nearly 0, and $(PO_4^{3-}–SO_4^{2-})/Ca^{2+}$, nearly 1, were consistent with the XRD assignment.

Possible explanations for the DCPD formation in the neutral solution are the following two. 1) A formation of a hydrated compound in an aqueous solution generally preferred, possibly due to kinetic and thermodynamic reasons, as a preferential formation of DCPD is in fact observed under many physiological, geochemical and laboratory conditions [38]. 2) Gypsum and DCPD show crystallographic and structural similarities [41] and many researches about crystallizations in gypsum-DCPD system have been reported [42-46]. An epitaxial effect between gypsum and DCPD might make it possible to form nuclei of DCPD, instead of HAp, even under a neutral condition. The more the phosphatization reaction of the w-Gyp proceeded, the lower pH get to, providing a more desirable condition for the DCPD formation.

Figure 9(b), XRD patterns after the phosphatization at 100 °C in the neutral solution, shows the initial DCPD formation and the following formation of DCPA as well as HAp. The DCPA formation would be explained in the same way as described above, and the HAp formation was general reaction at hydrothermal conditions which is accelerated with increasing in reaction temperature.

Figure 10 shows XRD patterns of the w-Gyp after the phosphatization in the weakly basic solution at 50, 100 or 200 °C for up to 72 h. These results would be explained in basically the same way as described above except for HAp and octacalcium phosphate pentahydrate (OCP, ICDD-26-1056) formations at 50 °C treatment (Fig. 10(a)). A formation of HAp is generally promoted in neutral to weakly basic conditions; however, a

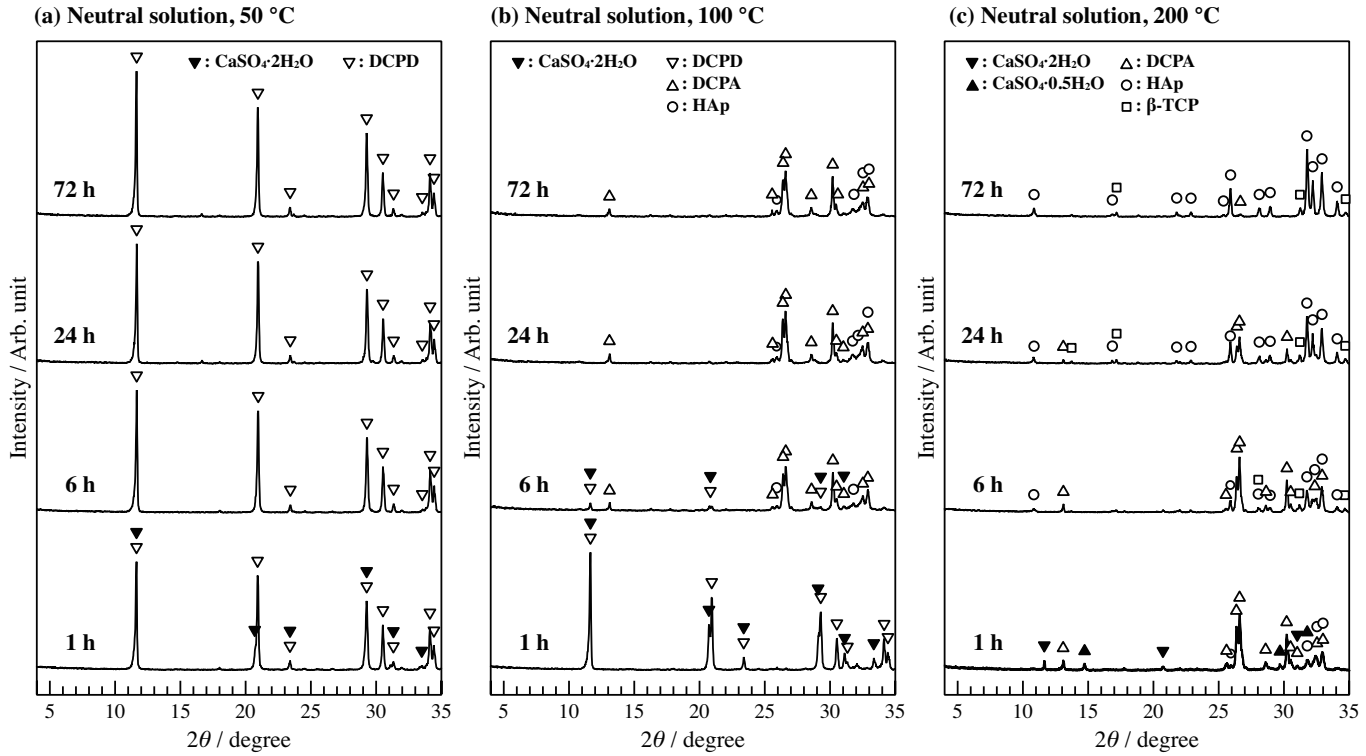

Figure 9. Powder X-ray diffraction patterns of w-Gyp after phosphatization in neutral ammonium phosphate salt solution at 50, 100 or 200 °C for up to 72 h.

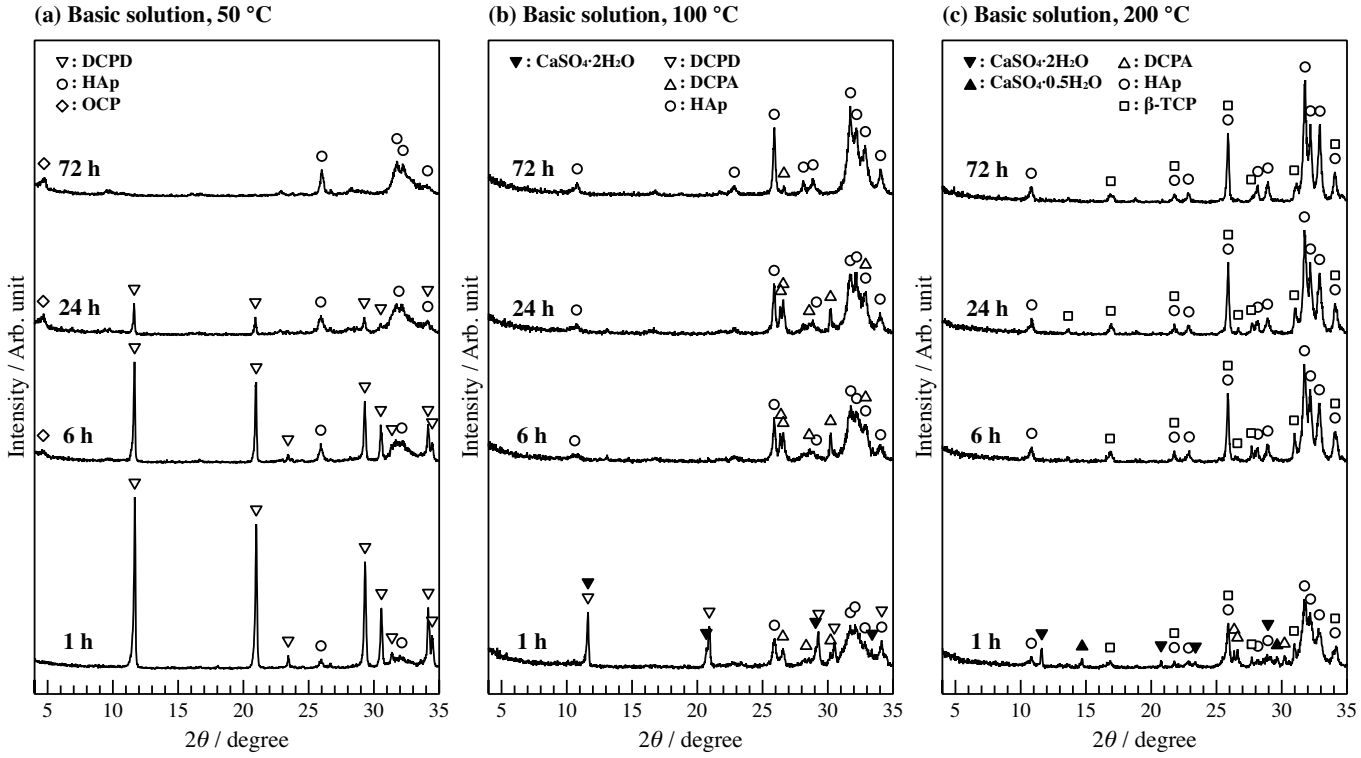

Figure 10. Powder X-ray diffraction patterns of w-Gyp after phosphatization in weakly basic ammonium phosphate salt solution at 50, 100 or 200 °C for up to 72 h.

crystal growth is not promoted at lower temperature than 100 °C. In addition, the crystal growth of HAp was inhibited by presence of Mg in the w-Gyp. Thus, all HAp peaks were broadened due to low crystallinity as shown in Fig. 10(a). In the meantime, although amorphous calcium phosphate, which could change into HAp via OCP, was barely formed in the conditions, low crystalline calcium phosphates might allow the formation of OCP as a precursor of HAp. With increasing in phosphatization temperature, HAp crystallinity increased with acceleration of the crystal formation and growth and no OCP was detected (Figs. 10(b,c)). Under 100 °C in basic conditions, DCPA were coexisted with HAp. The formation of DCPA would be due to stabilization of DCPA by sulfate-acidic condition by sulfate dissolution through accelerated HAp formation. Co-existence of β-TCP with HAp were found in the precipitates obtained under 200 °C and basic condition. After the 6-h treatment, DCPA disappeared by promotoion of crystal growth of HAp and β-TCP. Magnesium, contained in the w-Gyp, is known an inhibitor of HAp crystal formation and growth [47-49], and at lower temperature, loose crystal structure of lower crystalline HAp might allow the presence of Mg^{2+} in surroundings of HAp crystals; however, Mg^{2+} was excluded from HAp crystals with a formation of β-TCP, which structure is stabilized by Mg^{2+} incorporation [50, 51]. Peaks of β-TCP were not actually detected in the results for the c-Gyp phosphatized under the same condition (data was not shown).

The w-Beads were also phosphatized for 72 h at various pH and temperature in the same way as the w-Gyp phosphatization. Spherical shapes of the beads before the phosphatization were maintained after 72-h treatment except for them treated under conditions at 100 and 200 °C, and pH 4. Crystal phases of the spherical beads were almost the same as the phosphatized powders as shown above with slight differences in ratios among the crystal phases resulted from the difference in reaction rates between bead and powder. Thus, calcium phosphate beads with various calcium phosphates, such as HAp, DCPD, DCPA and their mixtures, were obtained by the phosphatization treatment of the w-Beads. These calcium phosphate beads have possibilities to be used as environmental purification materials and it might enable economical utilization of the w-Gyp.

4. Conclusion

The present study showed the fabrication method of spherical beads composed of various calcium phosphates from spherical beads of the waste gypsum. The waste gypsum powder collected from powdered waste gypsum board (w-Gyp) was gypsum ($CaSO_4 \cdot 2H_2O$) with some inorganic and organic impurities and dehydrated to bassanite ($CaSO_4 \cdot 0.5H_2O$) by heat treatment at 120 °C. The w-Gyp were phosphatized to various calcium phosphates, dicalcium phosphate dihydrate, dicalcium phosphate anhydrous or hydroxyapatite with a small amount of β-tricalcium phosphate depending on the treatment conditions, pH and temperature. Spherical beads composed of these calcium phosphates were also fabricated with slight differences in calcium phosphate ratios in comparison to phosphatized powders. The fabrication of calcium phosphate beads from the w-Gyp enables novel uses of waste gypsum boards, for instance, efficient components control for environmental purifications.

Acknowledgment

This work was financially supported by the Revitalization Promotion Program (A-STEP) (No. 241FT0375) of Japan Science and Technology Agency (JST).

References

[1] Gypsum Board Association of Japan, Gypsum board handbook (2012) (in Japanese).
[2] T. Yasue, Challenge to recycle society by resources recycling of waste gypsum materials, J. Soc. Inorg. Mater. Japan, 7 (2000) 492-502 (in Japanese).
[3] Y. Kojima, T. Yasue, Synthesis of large plate-like gypsum dihydrate from waste gypsum board, J. Eur. Ceram. Soc., 26 (2006) 777-783.
[4] Y. Kojima, S. Funada, T. Yasue, Production of gypsum hardened body contained active carbon from waste gypsum

board and its ad[sorption property, J. Soc. Inorg. Mater. Japan, 11 (2004) 212-218 (in Japanese).
[5] T. Kamei, A. Ahmed, K. Ugai, Durability of soft clay soil stabilized with recycled bassanite and furnace cement mixtures, Soils Found., 53 (2013) 155-165.
[6] S. Inazumi, H. Sano, M. Yamada, Estimation of gypsum hemihydrate content in recycled gypsums derived from gypsum boards, J. Mater. Cycle Waste Manag., 18 (2016) 168-176.
[7] S. Furuta, H. Katsuki, S. Komarneni, Removal of lead ions using porous hydroxyapatite from gypsum waste, J. Ceram. Soc. Japan, 108 (2000) 315-317.
[8] A. Aklil, M. Mouflih, S. Sebti, Removal of heavy metal ions from water by using calcined phosphate as a new adsorbent, J. Hazard. Mater., 112 (2004) 183-190.
[9] I. Smičiklas, S. Dimović, I. Plećaš, M. Mitrić, Removal of Co2+ from aqueous solutions by hydroxyapatite, Water Res., 40 (2006) 2267-2274.
[10] M. He, H. Shi, X. Zhao, Y. Yu, B. Qu, Immobilization of Pb and Cd in contaminated soil using nano-crystallite hydroxyapatite, Procedia Environ. Sci., 18 (2013) 657-665.
[11] S.M. Mousa, N.S. Ammar, H.A. Ibrahim, Removal of lead ions using hydroxyapatite nano-material prepared from phosphogypsum waste, J. Saudi Chem. Soc., 20 (2016) 357-365.
[12] S. Lazić, Ž. Vuković, Ion exchange of strontium on synthetic hydroxyapatite, J. Radioanal. Nucl. Chem., 149 (1991) 161-168.
[13] Y. Nishiyama, T. Hanafusa, J. Yamashita, Y. Yamamoto, T. Ono, Adsorption and removal of strontium in aqueous solution by synthetic hydroxyapatite, J. Radioanal. Nucl. Chem., 307 (2016) 1279-1285.
[14] H. Monma, S. Ueno, Uptake of fluoride ion by octacalcium phosphate and related calcium salts, Gypsum & Lime, 1981 (1981) (in Japanese).
[15] M. Tafu, T. Chohji, Reaction between calcium phosphate and fluoride in phosphogypsum, J. Eur. Ceram. Soc., 26 (2006) 767-770.
[16] M. Tafu, T. Masutani, Y. Takemura, T. Toshima, T. Chohji, Effect of hydroxyapatite on reaction of dicalcium phosphate dihydrate (DCPD) and fluoride ion, Bioceram. Dev. App., S1 (2013).
[17] Y. Takemura, M. Kikuchi, M. Tafu, T. Toshima, T. Chohji, Reactivity improvement of dicalcium phosphate dihydrate with fluoride for its removal from waste and drinking water, Univers. J. Mater. Sci., 4 (2016) 60-64.
[18] S. Furuta, H. Katsuki, S. Komarneni, Porous hydroxyapatite monoliths from gypsum waste, J. Mater. Chem., 8 (1998) 2803-2806.
[19] H. Katsuki, S. Furuta, S. Komarneni, Microwave- versus conventional-hydrothermal synthesis of hydroxyapatite crystals from gypsum, J. Am. Ceram. Soc., 82 (1999) 2257-2259.
[20] Y. Suzuki, S. Matsuya, K. Udoh, M. Nakagawa, Y. Tsukiyama, K. Koyano, K. Ishikawa, Fabrication of hydroxyapatite block from gypsum block based on $(NH_4)_2HPO_4$ treatment, Dent. Mater. J., 24 (2005) 515-521.
[21] S. Yasuike, H. Shimogaki, Synthesis and adsorption ability of hydroxyapatite made of recycled gypsum and phosphorus recovery from sewage sludge ash, J. Soc. Inorg. Mater. Japan, 15 (2008) 209-218.
[22] R. Lowmunkong, T. Sohmura, Y. Suzuki, S. Matsuya, K. Ishikawa, Fabrication of freeform bone-filling calcium phosphate ceramics by gypsum 3D printing method, J. Biomed. Mater. Res. Part B Appl. Biomater., 90B (2009) 531-539.
[23] H.P. Kurz, G. Münz, The influence of particle size distribution on the flow properties of limestone powders, Powder Technol., 11 (1975) 37-40.
[24] Y. Arai, From advancing researches on calcium salt in recent fifty years - Focusing on deposit and growth of crystal in aqueous solution, J. Soc. Inorg. Mater. Japan, 7 (2000) 363-384 (in Japanese).
[25] R.R. West, W.J. Sutton, Thermography of gypsum, J. Am. Ceram. Soc., 37 (1954) 221-224.
[26] J. Dweck, P.M. Buchler, A.C.V. Coelho, F.K. Cartledge, Hydration of a Portland cement blended with calcium carbonate, Thermochim. Acta, 346 (2000) 105-113.
[27] K.G. Wakili, E. Hugi, L. Wullschleger, T.H. Frank, Gypsum board in fire - Modeling and experimental validation, J. Fire Sci., 25 (2007) 267-282.
[28] K.G. Wakili, E. Hugi, Four types of gypsum plaster boards and their thermophysical properties under fire condition, J. Fire Sci., 27 (2009) 27-43.
[29] D.A. Kontogeorgos, M.A. Founti, Gypsum board reaction kinetics at elevated temperatures, Thermochim. Acta, 529 (2012) 6-13.
[30] J. Dweck, E.I.P. Lasota, Quality control of commercial plasters by thermogravimetry, Thermochim. Acta, 318 (1998) 137-142.
[31] P. Aggarwal, D. Dollimore, K. Heon, Comparative thermal analysis study of two biopolymers, starch and cellulose, J. Thermal Anal., 50 (1997) 7-17.
[32] D. Freyer, W. Voigt, Crystallization and phase stability of $CaSO_4$ and $CaSO_4$-based salts, Monats. Chem., 134 (2003) 693-719.
[33] J.C. Elliott, General chemistry of the calcium phosphates, in: Structure and chemistry of the apatites and other calcium orthophosphates, Elsevier, Amsterdam, 2013, pp. 1-62.
[34] G. Vereecke, J. Lemaître, Calculation of the solubility diagrams in the system $Ca(OH)_2$-H_3PO_4-KOH-HNO_3-CO_2-H_2O, J. Cryst. Growth, 104 (1990) 820-832.
[35] L. Amathieu, R. Boistelle, Crystallization kinetics of gypsum from dense suspension of hemihydrate in water, J. Cryst. Growth, 88 (1988) 183-192.
[36] M. Adachi, A. Tanimoto, On the equations represented solubility of calcium sulfate in pure water, Gypsum & Lime, 1975 (1975) 63-72 (in Japanese).
[37] A.A. Hanna, A.I.M. Akarish, S.M. Ahmed, Phosphogypsum: part I: Mineralogical, thermogravimetric, chemical and infrared characterization, J. Mater. Sci. Technol., 15 (1999) 431-434.
[38] R.A. Young, W.E. Brown, Structures of biological minerals, in: G.H. Nancollas (Ed.) Biological mineralization and demineralization, Springer-Verlag, Berlin, 1982, pp. 101-141.
[39] T. Ozawa, T. Ujiie, K. Tamura, Dehydration of calcium hydrogenphosphate dihydrate in water, Nippon Kagaku Kaishi, 1980 (1980) 1352-1357 (in Japanese).
[40] K. Setoyama, S. Takahashi, Crystal phase and shape control of gypsum, Inorg. Mater., 2 (1995) 498-505 (in Japanese).
[41] W.M.M. Heijnen, P. Hartman, Structural morphology of gypsum ($CaSO_4 \cdot 2H_2O$), brushite ($CaHPO_4 \cdot 2H_2O$) and pharmacolite ($CaHAsO_4 \cdot 2H_2O$), J. Cryst. Growth, 108 (1991) 290-300.
[42] C. Rinaudo, A.M. Lanfranco, M. Franchini-Angela, The system $CaHPO_4 \cdot 2H_2O$-$CaSO_4 \cdot 2H_2O$: crystallizations from calcium phosphate solutions in the presence of SO_4^{2-}, Journal of Crystal Growth, 142 (1994) 184-192.
[43] C. Rinaudo, A.M. Lanfranco, R. Boistelle, The gypsum-brushite system: crystallization from solutions poisoned by phosphate ions, J. Cryst. Growth, 158 (1996) 316-321.
[44] A. Hina, G.H. Nancollas, M. Grynpas, Surface induced constant composition crystal growth kinetics studies. The brushite–gypsum system, J. Cryst. Growth, 223 (2001) 213-224.
[45] A.J. Pinto, A. Jimenez, M. Prieto, Interaction of phosphate-bearing solutions with gypsum: Epitaxy and induced twinning

of brushite ($CaHPO_4 \cdot 2H_2O$) on the gypsum cleavage surface, Am. Mineral., 94 (2009) 313-322.
[46] A.J. Pinto, E. Ruiz-Agudo, C.V. Putnis, A. Putnis, A. Jiménez, M. Prieto, AFM study of the epitaxial growth of brushite ($CaHPO_4 \cdot 2H_2O$) on gypsum cleavage surfaces, Am. Mineral., 95 (2010) 1747-1757.
[47] H. Ding, H. Pan, X. Xu, R. Tang, Toward a detailed understanding of magnesium Ions on hydroxyapatite crystallization inhibition, Cryst. Growth Des., 14 (2014) 763-769.
[48] N.C. Blumenthal, Mechanisms of inhibition of calcification, Clin. Orthop. Relat. Res., 247 (1989) 279-289.
[49] M.H. Salimi, J.C. Heughebaert, G.H. Nancollas, Crystal growth of calcium phosphates in the presence of magnesium ions, Langmuir, 1 (1985) 119-122.
[50] B. Dickens, L.W. Schroeder, W.E. Brown, Crystallographic studies of the role of Mg as a stabilizing impurity in β-$Ca_3(PO_4)_2$. I. The crystal structure of pure β-$Ca_3(PO_4)_2$, J. Solid State Chem., 10 (1974) 232-248.
[51] S. Kannan, J.M. Ventura, J.M.F. Ferreira, Aqueous precipitation method for the formation of Mg-stabilized β-tricalcium phosphate: An X-ray diffraction study, Ceram. Int., 33 (2007) 637-641.